Experimental Study of Granular Compaction Dynamics at Different Scales: Grain Mobility, Hexagonal Domains, and Packing Fraction

G. Lumay and N. Vandewalle

GRASP, Département de Physique, Université de Liège, B-4000 Liège, Belgium

(Received 26 January 2005; published 7 July 2005)

We present an original experimental study of the compaction dynamics for two-dimensional granular systems. Compaction dynamics is measured at three different scales: the macroscopic scale through the normalized packing fraction $\tilde{\rho}$, the mesoscopic scale through the normalized fraction $\tilde{\phi}$ of hexagonal domains in the system, and the microscopic scale through the grain mobility μ. Moreover, the hexagonal domains are found to obey a growth process dominated by the displacement of domain boundaries. A global picture of compaction dynamics relevant at each scale is proposed.

DOI: 10.1103/PhysRevLett.95.028002 PACS numbers: 45.70.Cc, 64.70.Kb

Granular matter has been the subject of numerous studies since the last decade [1–3]. The packing fraction of those materials is a relevant parameter for a broad range of applications. A way to reduce the costs for the manipulation of such granular materials is to increase the packing fraction ρ. This can be achieved by tapping or vibrating the vessel containing the grains.

Various experimental studies [4–7] have emphasized the complexity of the slow compaction dynamics. Different laws have been proposed for the increasing packing fraction ρ of a granular material with the number n of taps. Since both initial ρ_0 and final ρ_∞ packing fractions depend on experimental conditions, a normalized parameter is defined as $\tilde{\rho} = (\rho - \rho_0)/(\rho_\infty - \rho_0)$, with $0 \leq \tilde{\rho} \leq 1$.

It has been proposed in Ref. [8], among others, that the packing fraction obeys an inverse logarithmic law

$$\tilde{\rho}(n) = 1 - \frac{1}{1 + B \ln(1 + \frac{n}{\tau})}, \tag{1}$$

where B and τ are dimensionless parameters. Opposite to the inverse logarithmic law, the Kohlrausch-Williams-Watts (KWW)'s law $\tilde{\rho}(n) = 1 - \exp(-(n/\tau)^{\beta})$ has the advantage to fit an observed saturation of the density [9,10]. The parameters τ and β correspond, respectively, to a characteristic tap number and to the stretching of the exponential.

Some theoretical models of compaction dynamics [11] are based on a relationship between the mobility μ of the grains and the packing fraction ρ. The mobility is a local property of each grain that corresponds to the grain ability to move in its nearest neighborhood inside the packing. The mobility is assumed to vanish when the packing fraction ρ reaches its asymptotical value ρ_∞. For highly packed hard-sphere suspensions, theoretical and experimental studies [12] suggested that the average mobility vanishes as a power law. However, Boutreux and de Gennes [13] argued that the logarithmic compaction dynamics [Eq. (1)] is related to the Vogel-Fulcher law

$$\mu = \mu_0 \exp\left(-\frac{c}{1 - \tilde{\rho}}\right), \tag{2}$$

where c represents some decay rate of the grain mobility near ρ_∞. The Vogel-Fulcher (2) law is derived from a Poisson distribution of voids in the system.

The slow dynamics of granular compaction has also been described by a cluster model [14]. A cluster is defined by grains that are ideally packed. The granular material is considered as a system of various clusters competing with a random environment. Vibrations cause the slow growth of the clusters. The relevant parameter is the fraction ϕ of grains ideally packed. As for the packing fraction ρ, this cluster parameter could also be normalized to vary between 0 to 1.

Therefore, compaction dynamics could be viewed through three different scales: the macroscopic scale ($\tilde{\rho}$), the mescoscopic scale ($\tilde{\phi}$), and the microscopic scale (μ). The relevant questions are thus the following: Is it possible to measure the grain mobility and the cluster formation? What are the experimental dynamical laws for $\tilde{\phi}$ and μ? What are the relationships between the different parameters describing compaction at different scales?

In this Letter, we present an experimental study of compaction for spherical particles confined between two parallel plates. This 2D granular system allows mobility and cluster measurements by tracking the grain position or motion during successive taps. Our experimental results relate the characteristics of granular packings at various scales. One should note that, to our knowledge, our work is the first experimental study of compaction focusing on both grain mobilities and clusters.

Let us describe the experimental setup. Spherical metallic particles are placed between two parallel plates. The number of particles is typically $N \approx 2000$. The mean bead diameter is $D = 2.4$ mm, with a polydispersity smaller than 3.6%. The distance between both plates is slightly greater than the particle diameter. The width of the pile is 58 mm ($\approx 25D$) and the mean height is 170 mm ($\approx 70D$). A

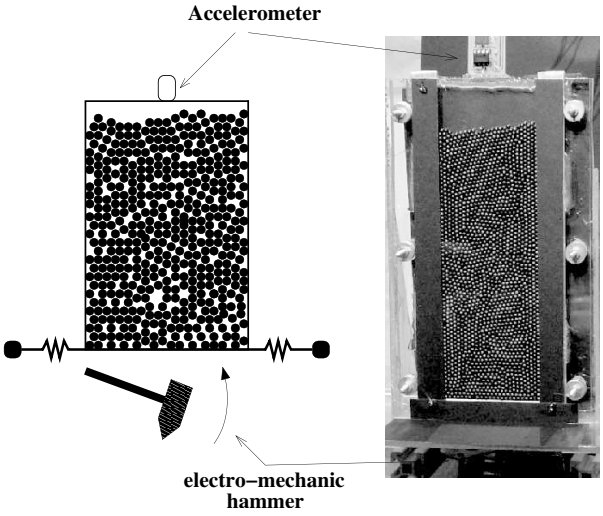

FIG. 1. A sketch (left) and a picture (right) of our experimental setup. Approximately 2000 beads are placed between two parallel plates. An electromechanic hammer is placed below the pile and is tuned by a microcontroller. An accelerometer is placed on the vessel to measure the acceleration experienced by the whole system.

sketch and a picture of the setup are given in Fig. 1. To produce the successive taps, an electro-mechanic hammer is placed below the container. The hammer is tuned by a micro-controller that can adjust the intensity, the number and the frequency of the taps. The acceleration experienced by the system at each tap is measured with the help of an accelerometer connected to an oscilloscope. During one tap, the system undergoes a short peak of acceleration (the width of the peak is 0.25 ms and the maximum intensity is 15 g) and some damped oscillations during 2 ms. Two successive taps are separated by 500 ms. This time is longer than the relaxation time of the system after each acceleration peak.

The pile is illuminated with a single light source. In such a way, the center of each particle appears bright on the pictures taken by a high-resolution CCD camera. The area of a grain corresponds to about 150 pixels on a picture. The camera can record an image of the packing after each tap. The position of each grain in the packing is later determined by image analysis. All grain positions are tracked by studying the correlations between successive images [15]. Figure 2 presents a part of the pile after numerical treatment of the pictures and for different values of the tap number n. The global packing fraction ρ of the pile is the ratio between the total area of the grains ($N\pi D^2/4$) and the total area of the packing. The latter area is evaluated by determining the positions of the particles being placed on the top of the heap.

Since the dynamics of the system slows down with the number of taps n, we recorded images of the system only for $n = 2^i$ with $i = 1, 2, \ldots, 16$. The maximum number of taps in our experiments is $n = 65\,536$.

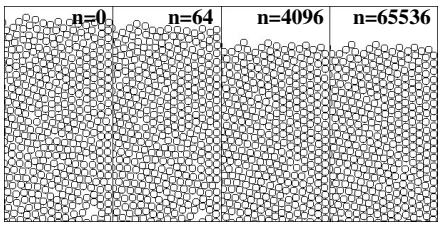

FIG. 2. A part of the pile after image analysis. Different values of the tap number n are illustrated. For $n = 0$, disorder is observed. When n increases, some hexagonal domains appear and grow thereafter. One should note that after $n = 65\,536$ taps, a few defects are still observed in the hexagonal structure.

We have repeated the experiment many times for statistical reasons. Obviously, small changes in the initial configurations of the packing give different values for ρ_0 and ρ_∞. Nevertheless, measurements of $\rho_0 = 0.825 \pm 0.002$ are reproducible. The last measurement $\rho(65\,536)$ of each series is assumed to be the asymptotic value $\rho_\infty = 0.862 \pm 0.004$. This value is slightly smaller than the 2D hexagonal packing fraction $\rho_h \simeq 0.91$. This difference can be explained by the presence of defects due to edge effects, by the presence of trapped defects, and by the small polydispersity of the grains. It is important to note that, in this experiment, we do not observe any convection, contrary to others [9,10].

The evolution of the normalized packing fraction $\tilde{\rho}$ as a function of the tap number n is presented in Fig. 3. Four different experiments are represented. After 65 536 taps, the saturation of the packing fraction is clearly obtained. One should note the collapse of all data sets when considering $\tilde{\rho}$ instead of ρ.

Since all the grain positions (x_i, y_i) are determined, it is possible to measure the displacement δ_i of the grain i during a tap: $\delta_i = \sqrt{\delta x_i^2 + \delta y_i^2}/N_{\text{tap}}$, N_{tap} being the number of taps realized between two successive pictures. A

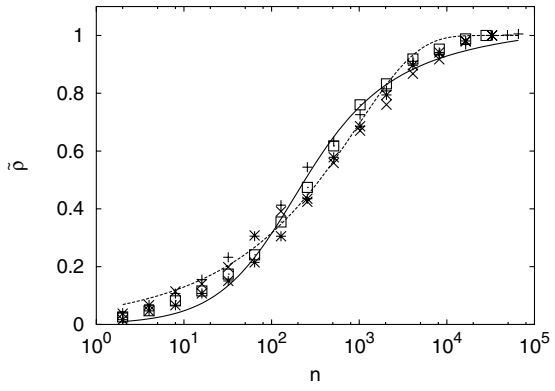

FIG. 3. Four typical curves (squares, circles, triangles, and crosses) giving the normalized packing fraction $\tilde{\rho}$ as a function of the tap number n. The solid curve is a fit using Eq. (1). The dashed curve is a fit using Eq. (7).

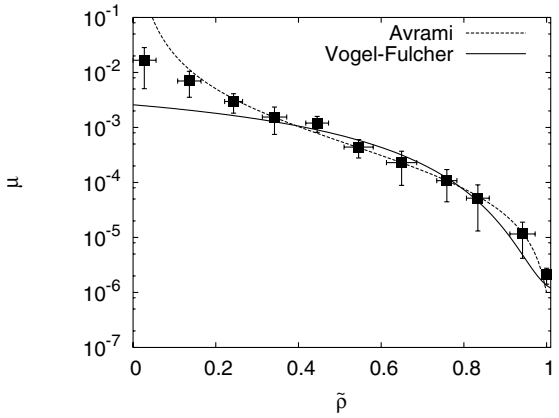

FIG. 4. Grain mobility μ as a function of the normalized packing fraction $\tilde{\rho}$. These results come from an average over various experiments. Error bars are indicated. The continuous curve is a fit of the Volger-Fulcher law [Eq. (2)]. The dashed curve is a fit with the Avrami law [Eq. (8)].

dimensionless average mobility μ can be defined from the ratio between particle displacements δ_i and particle diameters D. One has

$$\mu = \frac{1}{N}\sum_{i=1}^{N}\frac{\delta_i}{D}, \tag{3}$$

which can be easily computed. Figure 4 shows the decrease of the mobility μ according to the normalized packing fraction $\tilde{\rho}$. The nonzero value of the mobility for $\tilde{\rho} = 1$ is due to the finite spatial resolution of the camera and uncertainties on grain positions. These experimental results can be fitted by the Vogel-Fulcher law with $\mu_0 = 0.015 \pm 0.008$ and $c = 2.1 \pm 0.3$. The agreement is good for high values of the normalized packing fraction ($\tilde{\rho} > 0.3$). By considering that the variation of the packing fraction induced by a tap is proportional to the grain mobility, one has

$$\frac{\partial\tilde{\rho}}{\partial n} = k\mu, \tag{4}$$

where k is a constant. Injecting the Volger-Fulcher law in this equation leads to a solution [13] that corresponds to the inverse logarithmic law (1). The latter law correctly fits the data of Fig. 3, except at the end of the process when a saturation is observed.

Our image analysis allows us to determine the number of neighbors for each grain. Two grains are neighbors if their centers are separated by less than $D + \epsilon$ with $\epsilon \ll D$. The slight parameter ϵ is required because of the small polydispersity of the grains and because of the uncertainties on the grains' position. Typically, $\epsilon \approx D/15$. Grains belonging to hexagonal domains, i.e., being in contact with six neighbors, are shown in Fig. 5. One should note that the grains located along the domain boundaries are not considered. As we can see in Fig. 5, the pile is initially

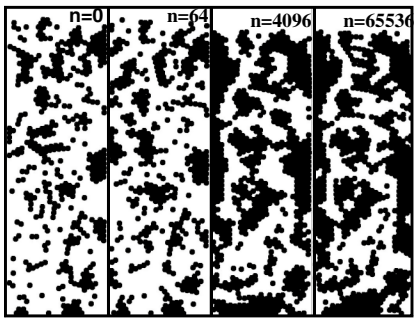

FIG. 5. Pictures of the pile for $n = 0$, 24, 4096, and 65 536. Only grains belonging to hexagonal domains are represented. The growth and fusion of domains are clearly seen.

disordered: the average coordination number is low. After a few taps, small hexagonal domains appear and start to grow. At the end of the compaction process, some defects still remain and create domain boundaries in the system. We have measured the number of hexagonal domains and their mean area. The normalized fraction $\tilde{\phi}$ of grains belonging to hexagonal domains in the system has been determined.

Figure 6 presents the normalized fraction $\tilde{\phi}$ of hexagonal domains as a function of the number of taps n. This growth is well described by the theoretical Avrami model

$$\tilde{\phi} = 1 - \exp\left(-\left(\frac{n}{\tau}\right)^{\alpha}\right), \tag{5}$$

where τ is a characteristic time [16]. The Avrami model describes the crystallization kinetics of various coexisting growing domains. The value of the parameter α depends on the nature of the growth. The experimental data are well fitted by this equation with an exponent $\alpha = 0.42 \pm 0.09$. In Avrami's theory, the value $\alpha = 1/2$ is a clear signature of a diffusion-controlled growth of hexagonal domains. This diffusive character could be understood as originating from the diffusion of defects along the borders of hexago-

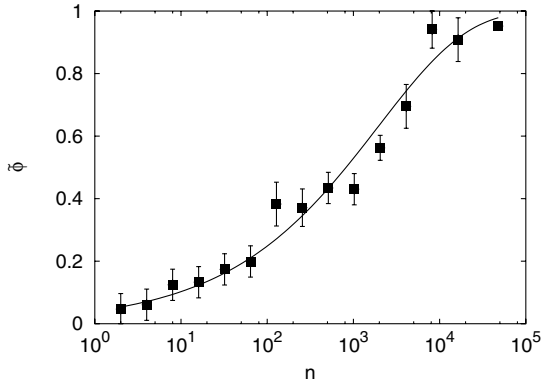

FIG. 6. Evolution of the normalized fraction $\tilde{\phi}$ of hexagonal domains as a function of the tap number n. The continuous curve is a fit using Eq. (5).

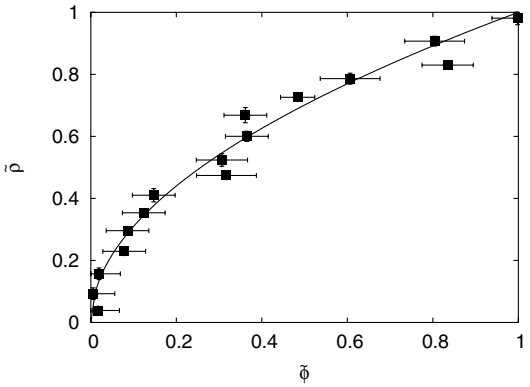

FIG. 7. Evolution of the normalized packing fraction $\tilde{\rho}$ according to the normalized hexagonal domains fraction $\tilde{\phi}$.

nal domains. Indeed, the grains not belonging to hexagonal domains are supposed to have a higher mobility than others as demonstrated in our experimental measurements.

In order to relate this mesoscopic view of compaction to the macroscopic measurements, we have drawn in Fig. 7 the fraction $\tilde{\rho}$ as a function of the fraction $\tilde{\phi}$. We have

$$\tilde{\rho} = \sqrt{\tilde{\phi}}, \tag{6}$$

which is illustrated by the continuous curve on the Fig. 7. This square root behavior means that the defects (leading to a lower density) are located only along the perimeter of the clusters. This relationship allows us to propose a new law for compaction dynamics

$$\tilde{\rho} = \sqrt{1 - \exp\left(-\sqrt{\frac{n}{\tau}}\right)}, \tag{7}$$

which is an alternative to the inverse logarithmic law (1) in 2D. This law could be adjusted to experimental data as seen in Fig. 3. The agreement is good. Furthermore, this law has the advantage to present a clear saturation for large n values, a saturation that was not accurately fitted by the law (1). The validity of this law has been checked with other tap intensities. If we assume that the normalized packing fraction $\tilde{\rho}$ increases linearly with the fraction of hexagonal domains $\tilde{\phi}$ (this assumption becomes reasonable when $0.3 < \tilde{\rho} < 1$), we recover KWW's law [9,10] for the evolution of $\tilde{\rho}$.

In order to obtain a compatible view of the crystallization phenomena with the grain motions, the law for the mobility becomes

$$\mu = -\frac{1}{k}\frac{1-\tilde{\rho}^2}{\tilde{\rho}\ln(1-\tilde{\rho}^2)}. \tag{8}$$

The results are fitted by this law in Fig. 4.

In summary, we have measured three physical quantities during granular compaction. They correspond to three different scales in the system. To our knowledge, it is the first time that such measurements have been performed. First, we have confirmed that the Vogel-Fulcher law (2) is a good candidate for describing grain mobilities in dense granular materials. Moreover, we have shown that granular compaction dynamics could be viewed as a slow process of crystallization driven by the diffusion of defects. The resulting laws (5), (7), and (8) are consistent with experimental data.

This work has been supported by Contract No. ARC 02/07-293. The authors thank Y. Bertho, H. Caps, S. Dorbolo, and F. Ludewig for valuable discussions.

[1] P. G. de Gennes, Rev. Mod. Phys. **71**, S374 (1999).
[2] H. M. Jaeger and S. R. Nagel, Rev. Mod. Phys. **68**, 1259 (1996).
[3] A. Kudrolli, Rep. Prog. Phys. **67**, 209 (2004).
[4] E. R. Nowak, J. B. Knight, E. Ben-Naim, H. M. Jaeger, and S. R. Nagel, Phys. Rev. E **57**, 1971 (1998).
[5] J. B. Knight, C. G. Fandrich, Chun Ning Lau, H. M. Jaeger, and S. R. Nagel, Phys. Rev. E **51**, 3957 (1995).
[6] P. Richard, M. Nicodemi, R. Delannay, P. Ribiere, and D. Bideau, Nat. Mater. **4**, 121 (2005).
[7] E. Caglioti, V. Loreto, H. J. Herrmann and M. Nicodemi, Phys. Rev. Lett. **79**, 1575 (1997).
[8] E. Ben-Naim, J. B. Knight, E. R. Nowak, H. M. Jaeger, and S. R. Nagel, Physica (Amsterdam) **123D**, 380 (1998).
[9] P. Philippe and D. Bideau, Europhys. Lett. **60**, 677 (2002).
[10] P. Ribière, P. Richard, D. Bideau, and R. Delannay, cond-mat/0503151.
[11] J. J. Arenzon and Y. Levin, Physica (Amsterdam) **325A**, 371 (2003).
[12] W. Gotze and L. Sjogren, Rep. Prog. Phys. **55**, 241 (1992); M. Tokuyama and I. Oppenheim, Physica (Amsterdam) **216A**, 85 (1995); W. van Megen, T. C. Mortensen, S. R. Williams and J. Muller, Phys. Rev. E **58**, 6073 (1998).
[13] T. Boutreux and P. G. de Gennes, Physica (Amsterdam) **244A**, 59 (1997).
[14] K. L. Gavrilov, Phys. Rev. E **58**, 2107 (1998).
[15] The tracking of the grains is based on an algorithm developed in the GRASP. This technique has already been used in N. Vandewalle, S. Trabelsi, and H. Caps, Europhys. Lett. **65**, 316 (2004).
[16] M. Avrami, J. Chem. Phys. **7**, 1103 (1939); M. Avrami, J. Chem. Phys. **8**, 212 (1940).